Pedestrian-level Air Flow and Ventilation around Adjacent Buildings in Step-up Configuration

Ayo, S. A.[1*]; Mohd-Ghazali, N.[2]and Bori I.[1]
[1]Department of Mechanical Engineering, Federal University of Technology Minna, Nigeria
[2]Faculty of Mechanical Engineering, UniversitiTeknologi Malaysia, 81310 Johor Bahru, Johor, Malaysia
E-mail: saayo1@gmail.com

Abstract
The outdoor air ventilation impact of a taller building at a downwind location in a layout of two adjacent buildings in different step-up configurations is presented in this paper. The criteria for ventilation assessment adopted are dimensionless parameters called velocity ratio (*VR*) and air ventilation rate (*AER*), and the parameters examined are the separation distance (W_V) between the buildings and the ratio of height of downwind building to that of upwind building, herein referred to as building height ratio (*HR*). A three-dimensional (3-D) numerical simulation employing the Computational Fluid Dynamics (*CFD*) technique based on Reynolds-Averaged Navier-Stokes (*RANS*) equation and Realizable *k-ε* turbulence model was used to study the turbulent flow field around various full-scale size configurations of the adjacent buildings. Results show that while *VR* generally increases with height ratio, it increases with separation distance until a certain maximum distance which depends on the height ratio. *AER* on the other hand generally increases with height ratio, but decreases with separation distance. The results indicate that greater air motion is induced at the pedestrian level as the height of the downwind building increases, and greater rate of air flow is exchanged between the buildings cavity and the surroundings. Based on the *VR* results obtained for the building configurations examined, a separation distance of between 18 m and 30 m is proposed for configurations $2.0 \leq HR \leq 3.0$, and between 18 m and 24 m for configurations *HR* = 1.0 and 1.5, to maximally invigorate the pedestrian-level air flow.

Keywords: Separation distance, Building height ratio, Adjacent buildings, Computational Fluid Dynamics, Outdoor air ventilation

Introduction
Ventilation of the outdoor environment around buildings is necessary for the thermal comfort and environmental health of the inhabitants in and around the buildings. Literatures (Buccolieri *et al.*, 2010; Hang *et al.*, 2011; Yuan *et al.*, 2014; Ayo *et al.*, 2015) have shown that the spacing distance between adjacent buildings can significantly influence the outdoor ventilation around the buildings. Ventilation has also been found to generally increase as the spacing distance between buildings increases. However, because of limitations to land availability there is the need to explore intermediate spacing distances which may engender acceptable ventilation around the buildings.

Most of existing research studies on wind flow characteristics around building groups focused on configurations in which the buildings are aligned and have uniform heights. The few studies on configurations with uneven canyons mainly adopted highly simplified models, such as two-dimensional (2-D) configurations and reduced scales, and are not with reference to actual wind data of an urban area. Such 2-D analysis does not capture the lateral turbulent flow features such as the finite-length canyon effects which cause intermittent vortices shedding at building corners. These effects are known to be responsible for the lateral advection from building corners to the mid-block region around which it creates a convergent zone

(Santamouris *et al*., 1999). Besides, in actual street canyons exchange of canyon air occurs both vertically through the canyon roof and laterally across the street opening, but in 2-D studies the exchange is only across the canyon roof. Thus, 2-D and 3-D results often differ from each other (Liu *et al*., 2004; Riain *et al*., 1998; Ahmad *et al*., 2005; Li *et al*., 2006).The limitations of 2-D study have also been mentioned by Chan *et al*. (2001) and Baik and Kim (1999).

The present study is aimed at assessing the effects of the variation of buildings height ratio and separation distance on the wind flow and air ventilation around different configurations of a typical two-building layout of the step-up configuration with a taller downwind building. It forms a part of the preliminary studies of a broad investigation being conducted into the blockage effects of tall buildings to wind flow and ventilation on arrays of low-rise buildings, aimed at formulating appropriate climatically oriented guidelines for building layout in an urban area.

Physical Model and Mathematical Formulation and Analysis

Computational Methods

Ventilation enhancement is most desirable for low-wind, hot and humid climates where people are more likely to suffer from thermal discomfort and problems related to low air quality. A typical low-wind suburban area of Kuala Lumpur the capital City of Malaysia was therefore considered for the study. From the ten-year climatic data of Subang Meteorological Station collected from Malaysia Meteorological Department, the City has a mean surface wind speed of about 1.52 m/s at a height of 10 m above the ground surface, a mean temperature of about 27.8^{o}C, and a maximum and minimum relative humidity of 98% and 38%, respectively. The wind data, after adjustment from the value at the open terrain of the Meteorological Station where it was monitored to the sub-urban terrain in which it is to be utilized, is used to develop a wind profile for the sub-urban area.

The study uses two building blocks, a low-rise building (A) and a high-rise building (B), to represent the two adjacent buildings. The buildings are of the single loaded long corridor type in which access to the rooms is located along one of the building walls. The dimensions of the buildings are in accordance with Bye-Law 42 of Malaysian Uniform Building Bye-Law (*UBBL*) 1984, 2006 edition. In order to ensure that the building wind blocking effects are not completely cancelled out at the mid-length of the street canyon by advection from the building corners, the length-to-height ratio of the uniform configuration, i.e. $L/H > 3$, and therefore above the short canyon classification according to Ahmad *et al*. (2005). The geometries of the individual blocks are shown in Fig. 1.

Building Configurations Examined

The outdoor ventilation effect of building ‘B’ located adjacent to building ‘A’ is examined by placing building B at a downwind location of building A in an atmospheric boundary layer. The layout of the two adjacent buildings is as shown in Fig. 2. Building A represents the low-rise building, while building B represents the high-rise building. However, the height of building B is increased from the height *H* of the low-rise building until it is in the high-rise configuration which has been defined as a building for which the height

H of building and building depth *D* are related as follows: *H* > *3D* (ASHRAE, 1997) or *2H/D* > 1 (Cook, 1990). The height *H* corresponds to the approximate height of common low-rise buildings for the low income earners found around Malaysia.

To examine the impact of the height of the downwind building at the pedestrian level around the upwind building, the height of building B (H_v) is varied while that of the building A is kept constant. The height of the downwind building B is varied from *H* = 12 m (equivalent to 4 storeys), the constant height of the low-rise building, to a maximum height H_{max}= 3*H* = 36 m (equivalent to 12 storeys), with a step-increase of ½*H*. The separation distance (W_v) between the two buildings is also varied from a minimum of ½*H* to 3*H* with a step-increase of 2*H*, to examine the impact of the distance between the buildings on the outdoor air ventilation. The configuration in which no high-rise building is present at the downwind location of the low-rise building, i.e. H_v = 0*H*, is used as reference. The different heights of building 'B' examined are therefore 0*H* (reference case), *H*, 1.5*H*, 2*H*, 2.5*H*, and 3*H*, while the separation distances between the buildings are 0.5*H*, *H*, 1.5*H*, 2*H*, 2.5*H*, and 3*H*. The constant increment of 0.5*H* on the separation distance between the buildings represent the combined 6 m minimum setback from the buildings stipulated by Malaysian Planning Guideline for Gated Community and Guarded Neighbourhood (GP022), 2010 edition, while the increment on the building height is to ensure the regime of flow varies from skimming flow for the smallest separation to wake interference flow for the largest. Ventilation is most important for this range of flow regimes. The different arrangements of the buildings yield a total of 31 configurations that were examined. The geometries of the individual building are shown in Fig. 3, while Fig. 4 shows the schematic diagrams of the different configurations examined.

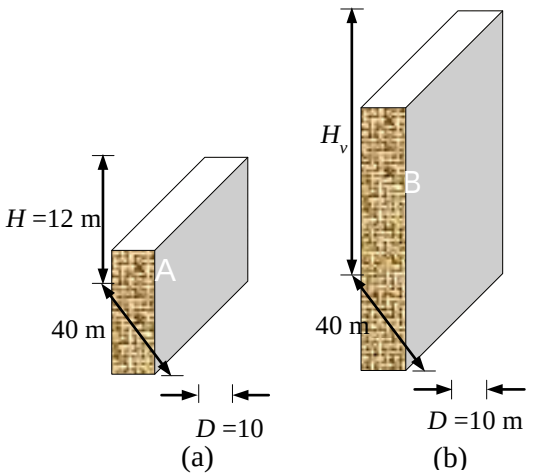

Fig. 1 Geometries of the individual building block; (a) Low-rise building, (b) High-rise building

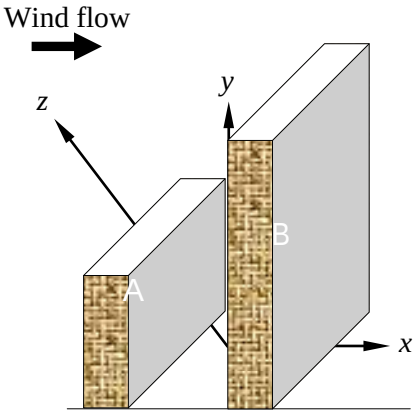

Fig. 2 Layout of the two adjacent buildings

Method of Solution

The present study examines the sensitivities of downwind building height and separation distance between the adjacent buildings to study the outdoor pedestrian-level flow and ventilation characteristics, employing a total of 31 configurations of the buildings layout. As a result, the most

appropriate solution method, in terms of cost and effort, which is by computational fluid dynamics (*CFD*) was considered. The applicable governing equations are therefore prescribed and solved for the relevant flow parameters for analysing the flow phenomenon.

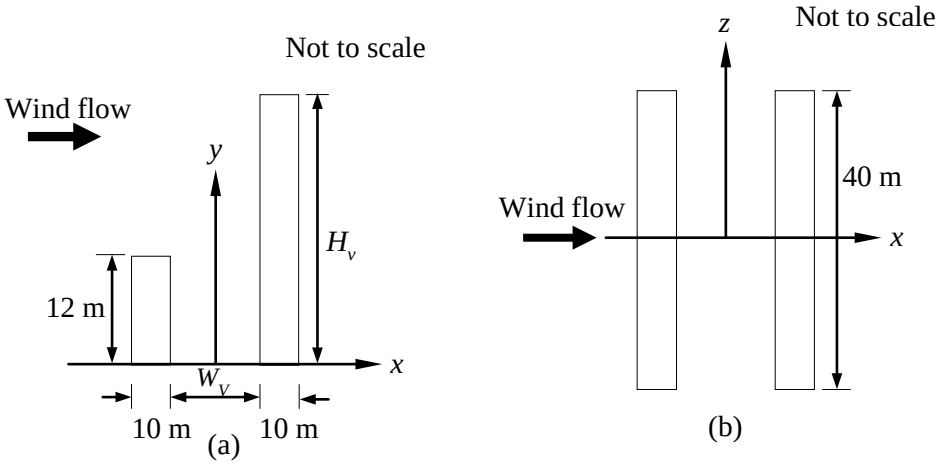

Fig. 3 Geometry of the two adjacent buildings showing (a) side view; (b) top view

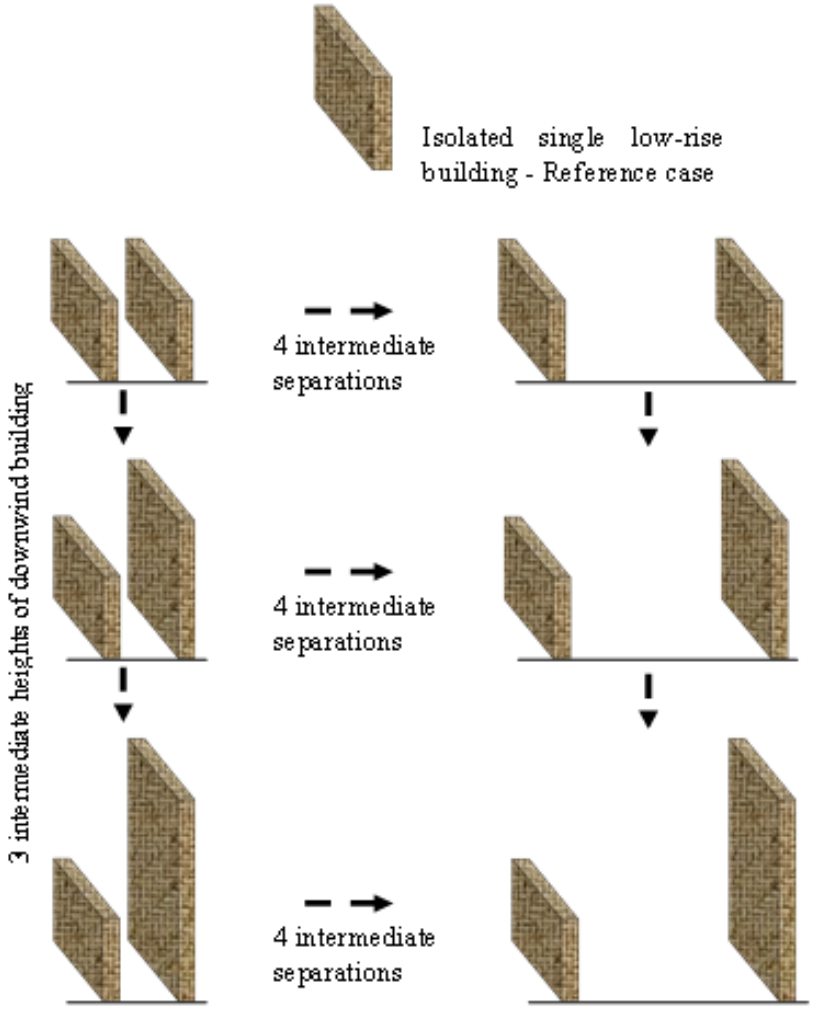

Fig. 4 Schematic diagrams of various configurations of the two adjacent buildings. Flow direction is from left to right

CFD Modelling

Wind flow in an urban area has been identified to occur in the turbulent flow regime (Raupach *et al*., 1991; Mills *et al*., 2010). For the building configurations employed in the current research, $Re_H = 695924.92$ (where Re_H is the Reynolds number based on the height of the low-rise building), which is well above the critical limits of between 3400 and 7500 observed for boundary layer developing over an urban surface (Mochida *et al*., 1994; Uehara *et al*., 2003).The isothermal flow is therefore described by the continuity and Navier-Stokes momentum equations. The full-scale sizes of the buildings are employed in the study, which is the realistic scenario for *CFD* simulations of physical processes. The implication, however, is the large computational domain, which was about 800 m in the stream wise direction for the larger domains, and the large number of meshes, which ranges between 3 million and 5 million that are required in the solution process. The solution procedure adopted, therefore, is based on the Reynolds Averaged Navier-Stokes (*RANS*) approach, with closure for the model equations obtained by the Realizable *k-ε* (*RKE*) turbulence model. The resulting equations are the mean form of continuity equation and momentum equation, and the transport equations of turbulent kinetic energy *k* and the dissipation rate of turbulent kinetic energy *ε,* expressed respectively as follows:

$$\frac{\partial \bar{U}_i}{\partial x_i} = 0 \tag{1}$$

$$\bar{U}_j \frac{\partial \bar{U}_i}{\partial x_j} = -\frac{1}{\rho}\frac{\partial \bar{P}}{\partial x_i} + \frac{\partial}{\partial x_j}\left(\nu \frac{\partial \bar{U}_i}{\partial x_j} - \overline{u_i'' u_j''}\right) \tag{2}$$

$$\bar{U}_i \frac{\partial k}{\partial x_i} = \frac{1}{\rho}\frac{\partial}{\partial x_i}\left\{\left(\mu + \frac{\mu_t}{\sigma_k}\right)\right\}\frac{\partial k}{\partial x_i} + \frac{1}{\rho}P_k - \varepsilon \tag{3}$$

$$\bar{U}_i \frac{\partial \varepsilon}{\partial x_i} = \frac{1}{\rho}\frac{\partial}{\partial x_i}\left\{\left(\mu + \frac{\mu_t}{\sigma_\varepsilon}\right)\right\}\frac{\partial \varepsilon}{\partial x_i} + C_1 S\varepsilon - C_2 \frac{\varepsilon^2}{k+\sqrt{\nu\varepsilon}} \tag{4}$$

where,

$\overline{u_i'' u_j''} = \frac{2}{3}k\delta_{ij} - \nu_t\left(\frac{\partial \bar{U}_i}{\partial x_j} + \frac{\partial \bar{U}_j}{\partial x_i}\right)$; $P_k = \nu_t\left(\frac{\partial \bar{U}_i}{\partial x_j} + \frac{\partial \bar{U}_j}{\partial x_i}\right)\frac{\partial \bar{U}_i}{\partial x_j}$; $\nu_t = \frac{\mu_t}{\rho}$; $\mu_t = \rho C_\mu \frac{k^2}{\varepsilon}$; $C_\mu = \frac{1}{A_0 + A_s\frac{kU^*}{\varepsilon}}$; $A_0 = 4.04$; $A_s = \sqrt{6}\cos\phi$; $\phi = \frac{1}{3}cos^{-1}\left(\sqrt{6}\,W\right)$; $W = \frac{S_{ij}S_{jk}S_{ki}}{\tilde{S}^3}$; $S_{ij} = \frac{1}{2}\left\{\frac{\partial \bar{U}_j}{\partial x_i} + \frac{\partial \bar{U}_i}{\partial x_j}\right\}$; $U^* = \tilde{S} = \sqrt{S_{ij}S_{ij}}$; $C_1 = max\left[0.43, \frac{\eta}{\eta+5}\right]$; $\eta = S\frac{k}{\varepsilon}$; $S = \sqrt{2S_{ij}S_{ij}}$. x_i is the Cartesian coordinates, $\bar{U}_i$ is the components of the mean velocity, u_i'' is the components of the fluctuating velocity, in the *x*-, *y*- and *z*-directions for *i* = 1, 2, 3 respectively; and $C_{1\varepsilon}$, C_2, σ_k, and σ_ε are model constants which have values as follows: $C_{1\varepsilon} = 1.44$, $C_2 = 1.9$, $\sigma_k = 1.0$, $\sigma_\varepsilon = 1.2$. The model equations are computed using the commercial *CFD* codes *ANSYS* Fluent 14.0 (Ansys, 2011).

Configuration of the Computational Domain

The computational domains were designed based on the recommendations of major *CFD* guidelines and past studies (Franke *et al*., 2004; Franke, 2006; Franke *et al*., 2008; Tominaga *et al*., 2008). In the guidelines, it is recommended that in the case of a single building the inflow boundary, the lateral and top boundaries are set 5*H* away from the windward face, the lateral and the top surfaces of the building, where *H* is the height of the building, while the outflow boundary is set at a distance ≥

10H from the leeward face of building in order to allow for the flow to have become fully redeveloped. For two or more buildings the reference height H is the height of the taller/tallest building and the distance of the inflow boundary should be from the windward face of the first building at the upwind location, while that of the outflow boundary should be from the leeward surface of the last building at the downwind location. Following from the recommendations, the reference height used in the current study is H_v, where H_v is the variable height of the taller upwind building. The outflow boundary is set $15H_v$ from the leeward surface of the downwind building as observed for most studies to ensure flow redevelopment. The computational domain is shown in Fig. 5.

Boundary Conditions

The mean surface wind speed monitored at the meteorological station, after adjustment to the terrain of the sub-urban area where the study is referenced, yields a reference mean wind speed of 0.92 m/s at a height of 10 m. The reference wind speed was used to develop a profile for velocity at the inflow of the computational domain. The inflow profiles for velocity, turbulent kinetic energy and dissipation rate of turbulent kinetic energy were specified employing the relations suggested by Richards and Hoxey (1993) following the recommendations of European Cooperative in the Field of Scientific and Technical Research (*COST*). The profiles are expressed, respectively, as follows:

$$U(y) = \frac{u^*_{ABL}}{\kappa} ln\left(\frac{y+y_0}{y_0}\right); k(y) = \frac{u^{*2}_{ABL}}{\sqrt{C_\mu}}; \varepsilon(y) = \frac{u^{*3}_{ABL}}{k(y+y_0)} \quad (5)$$

where κ ($\approx 0.4-0.42$) is the von Karman constant, $C_\mu (= 0.09)$ is a model constant of the Standard k-ε model, y_0 is the roughness parameter and $u^*_{ABL}$is the atmospheric boundary layer friction factor. The roughness parameter is specified asy_0= 0.02 m, which corresponds to a terrain of grassland according to the classification by Wieringer (1992), in order to locate the pedestrian-level evaluation height at the third or higher grid from the ground surface (Franke *et al*., 2007). The friction factor $u^*_{ABL}$is calculated as:

$$u^*_{ABL} = \frac{\kappa U_h}{ln\left(\frac{h+y_0}{y_0}\right)} \quad (6)$$

U_h being the reference velocity and h the height at which the reference velocity is specified.

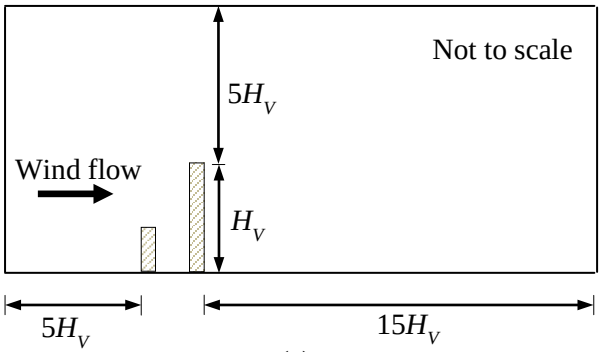

(a)

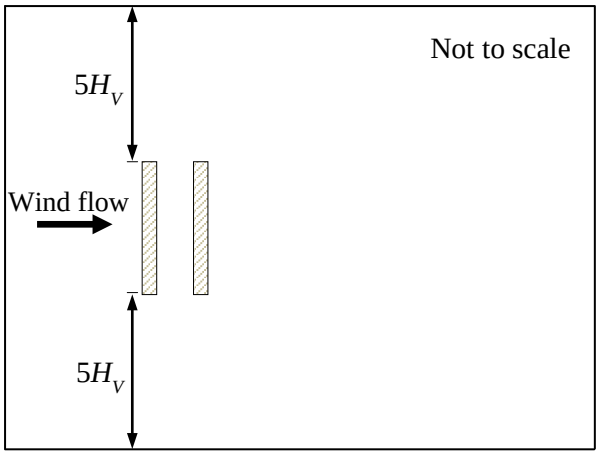

(b)

Fig. 5 Configuration of the computational domain for the layout of the two adjacent buildings (a) side view, (b) Plan

The downstream boundary conditions are specified by the outflow boundary conditions, setting the normal gradients of all variables to zero at the boundary, while the lateral and upper surfaces are assigned the inviscid wall conditions which set the normal velocity components and the normal gradients of tangential velocity components to zero at the surfaces.

The solid boundaries are treated by the wall-function based on the physical roughness height K_s of the surface for the wall-adjacent cell values of the flow parameters. For building surfaces normally considered as being aerodynamically smooth, the conditions are specified by the smooth wall condition. The wall-function for velocity, turbulent kinetic energy and dissipation rate of turbulent kinetic energy are therefore expressed respectively as follows:

$$\frac{U_p}{u^*} = \frac{1}{\kappa} ln\left(\frac{u^* y_p}{\nu}\right) + B;\;\; k_p = \frac{u^{*2}}{\sqrt{C_\mu}};\;\; \varepsilon_p = \frac{u^{*3}}{\kappa y_p} \qquad (7)$$

where U_p, k_p, ε_p are the wall-adjacent cell values of velocity, turbulent kinetic energy and dissipation rate of turbulent kinetic energy, respectively. y_p is the distance between the centre-point *P* of the near-wall cell and the surface, u^* is the friction factor, and *B* ($\approx 5 - 5.5$) is a universal constant.

With buildings as the main roughness elements of an urban surface, the ground surface is considered as a fully-rough surface. For the fully rough surface, the wall-function for mean velocity of the wall-adjacent cells can be expressed as (Fluent, 2005; Blocken *et al*., 2007)

$$\frac{U_p}{u^*} = \frac{1}{\kappa} ln\left(\frac{u^* y_p}{\nu C_S K_S^+}\right) + 5.43 \qquad (8)$$

where C_S with value in the interval [0; 1] is the roughness constant which accounts for the type of roughness and K_S^+ is the dimensionless physical roughness height. The wall-function for turbulent kinetic energy and dissipation rate of turbulent kinetic energy are defined as for the building wall surface.

Numerical Simulation

The computation of the governing equations (1) - (4) using the outlined boundary conditions was implemented by the commercial software *ANSYS* Fluent 14.0. The computational domain was discretized into unstructured tetrahedral grid elements by using *ANSYS* Meshing 14.0. The grid sizes were further refined around the building corners in order to capture the fine details of the flow parameters.The growth rate of the cells was maintained at below 1.2, while the aspect ratio was kept at between 0.5 and 20 (Ansys, 2011; Tominaga *et al*., 2008).

Grid sensitivity test was conducted in order to ensure mesh independence of the solution. The number of grid cells assigned to each domain depends on the size of the domain. The test was conducted by repeatedly refining the mesh sizes until the difference of the pedestrian-level area-average velocity values obtained for the last two consecutive mesh sizes was less than 5%, after which the lower grid number was selected for the domain. Because of the large number of configurations examined, for a particular separation distance, the test was conducted for the smallest and largest

domain sizes. The intermediate domain sizes not tested were then assigned grid cell numbers proportional to their sizes. The number of mesh elements range from 1.5 m for the single low-rise building to 3.5 m for the largest domain which was for the largest configuration with the tallest high-rise building.

The boundary conditions which set the normal velocity components and the normal gradients of tangential velocity components to zero at the lateral and top surfaces of the domain are implemented by specifying the zero shear condition at the surfaces. At the downstream boundary the flow condition is assumed to be fully developed, indicating that the longitudinal gradients of all variables are zero. This is implemented by specifying the outflow boundary condition in the solver. On the ground surface the wall function for fully rough surface for the mean velocity at the wall-adjacent cells expressed by equation (8) is implemented, while the wall-adjacent values for turbulent kinetic energy and the dissipation rate are implemented by equation (7). This is accomplished by specifying the terrain roughness height $y_0 = 0.02\,m$ and the surface roughness constant, $C_S = 1.0$. The wall-functions for smooth surface expressed by equation (7) are implemented for the building surfaces to calculate the wall adjacent values for velocity, turbulent kinetic energy and the dissipation rate of energy for the surfaces. In the solver this is by specifying the roughness height as zero.

The computation of the mathematical models was by the pressure-based solver, while the solution method for the pressure-velocity coupling was the Semi-Implicit Method for Pressure-Linked Equations (*SIMPLE*) algorithm. The method calculates the pressure by a guess-and-correct procedure on a staggered grid arrangement in which the three components of velocity are solved on different grids, while pressure, turbulent kinetic energy and dissipation rate of energy scalar variables are solved on the same grid. The second-order discretization scheme was adopted for pressure, while for momentum, turbulent kinetic energy and the dissipation rate, the quadratic interpolation for convection kinetics (*QUICK*) scheme (Leonard, 1979) was used. The profiles for the flow variables: velocity, turbulent kinetic energy and dissipation rate of turbulent kinetic energy at the inflow boundary, as represented by equations (5) and (6), were coded by user-defined functions (*udf*) in the solver. In order to control convergence of the iterations, a uniform scaled-residual set at 1 x 10^{-5} was employed for all variables. The computation was implemented on a network of interconnected 8 CPU × 6 Nodes Quad-Core AMD Opteron™ processor SunFire Systems of the UniversitiTeknologi Malaysia (UTM) Centre for Information and Communication Technology (CICT) Unit.

Air Ventilation Performance Criteria Adopted

The air ventilation performance of the various configurations of the buildings layout was assessed by two air ventilation indicators called velocity ratio (*VR*) and air exchange rate (*AER*). The wind velocity ratio is a dimensionless quantity that compares the velocity, V_P, at the pedestrian level (2 m above ground surface) with some reference velocity. It is defined according to according to Ng *et al.*. (2008) and Yim *et al.* (2009) as

$$VR = V_p/V_\infty \qquad (9)$$

For the present study the reference velocity, V_∞, is taken as the wind velocity at the gradient height (atmospheric boundary layer height).The air exchange rate denotes the volumetric air exchange per unit time (Xie *et al*., 2006) in the cavity between the buildings bounded at the top by the horizontal plane at a height of 12 m. Following Xie *et al.* (2006), for the 3-D

system, the mean positive *AER* ($\overline{AER}_+$) for air entering into the canyon across the boundaries can be expressed as

$$\overline{AER}_+ = \sum_{i=1}^{2} \int_{\Gamma} \bar{W}_+ d\Gamma \Big|_{side\ i} + \int_{\Gamma} \bar{V}_+ d\Gamma \Big|_{Top} + \sum_{i=1}^{3} \frac{1}{\sqrt{6}} \int_{\Gamma} \sqrt{k}\, d\Gamma \Big|_{plane\ i} \quad (10)$$

where, $\bar{W}_+$ and $\bar{V}_+$ are the mean positive transverse and vertical velocity components, w_+'' and v_+'' are the mean positive transverse velocity and vertical velocity fluctuations, and *k* the turbulent kinetic energy on the ventilation boundaries Γ. The breathing capacity, as determined by the *AER*, of the different configurations studied is made dimensionless by the volume of the canyon cavity between the buildings, and a time scale based on the height of the downwind building. The non-dimensionlizing volume parameter is therefore not a constant but changes as the separation distance between the buildings changes.

Validation of the CFD Model

The performance of the CFD model has been assessed in a previous study (Ayo *et al*., 2015) by comparing the simulation results of the model equations with experimental data from the wind tunnel experiment conducted by a working group of the Architectural Institute of Japan (*AIJ*) on the flow field around the model of a single high-rise building. The details are, however, highlighted here for ease of access to the information. The *AIJ* experiment was one of the series aimed at formulating guidelines for the *CFD* prediction of the pedestrian wind environment around buildings (Tominaga *et al*., 2008). The geometry of the building model has scale ratio 4: 4: 1 (height: width: depth), with a depth, *a* = 0.05 m. The geometry of the building model is as shown in Fig. 6.

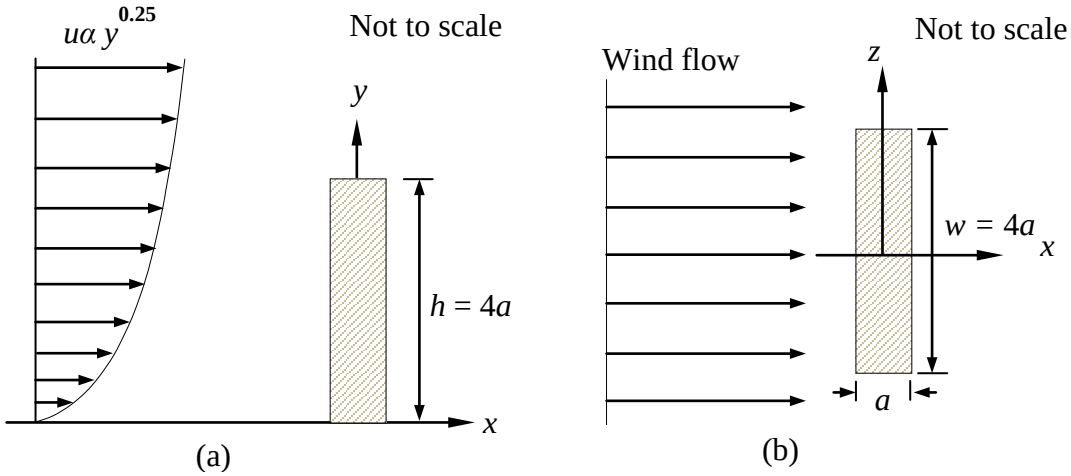

Fig. 6: Building model with the approach wind speed profile (a) Side view; (b) Top view

The wind tunnel used for the experiment has dimensions of the test section 1.65 m x 1.6 m x 1.65 m (width x height x length). Measurements of *x*-, *y*- and *z*-components of mean and instantaneous velocities were conducted using split-fibre anemometer. The wind velocities were taken around the building model at 109 points along the vertical plane of symmetry of the model and at 115 points on a horizontal plane at a

height of 12.5 mm from the base floor. At the inflow boundary, along the vertical line on the plane of symmetry the wind velocity measurements were conducted at 12 points. Fig. 7 shows the locations of the axes along which the wind velocity measurements were made. The velocity measurements were then used to determine the three components of velocity fluctuations and the turbulent kinetic energy at the various points. However, no graphical details of flow features such as streamlines and velocity vectors around the model were plotted.

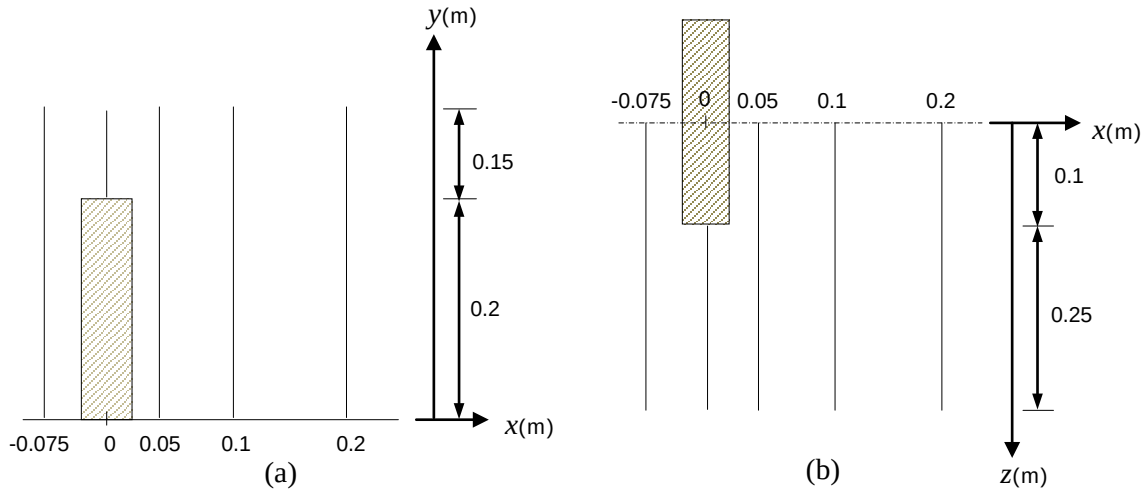

Fig. 7: Locations of measurement of wind profiles (a) on the vertical plane along the centreline of the building; (b) on the horizontal plane at y=0.0125m ($\frac{1}{16}h$). Direction of flow is from left to right

As for the main simulation, the computational domain for the *CFD* validation was also designed following recommendations of major *CFD* guidelines, with the inflow boundary, the lateral and top boundaries set 5*h* away from the building, while the outflow boundary was located 15*h* behind the building. At the inflow boundary of the computational domain, the profile of the wind determined in the wind tunnel experiment was replicated, while the data for turbulent kinetic energy and the rate of dissipation were represented with closely approximating functions. For the turbulent kinetic energy, k, at the inflow boundary, the profile data from the experiment was interpolated by a combination of closely approximating polynomial and exponential functions to obtain the function $k(y)$. Following recommendations from both the experiment and *AIJ* guidelines, the vertical profile for the dissipation rate of turbulent kinetic energy, $\varepsilon(y)$, was approximated by assuming local equilibrium between the production and dissipation rate of k, to yield an expression for the ε profile as follows (Tominaga *et al*., 2008; 2004):

$$\varepsilon(y) = C_{\mu}^{\frac{1}{2}} k(y) \frac{U_{ref}}{y_{ref}} \alpha \left(\frac{y}{y_{ref}}\right)^{(\alpha-1)} \qquad (11)$$

where $k\,(y)$ is the profile for k as approximated by the combination of the polynomial and exponential functions.

As for the main simulation also, the downstream boundary conditions were specified by zero normal gradients of all variables, while the lateral and upper surfaces were assigned the inviscid wall conditions. The boundary conditions for the ground surface was specified by the wall-function based on the logarithmic law for rough surface with roughness length determined in the experiment as y_0=

$9.6x10^{-5}$ m, while the building surfaces were specified by the smooth wall condition. In a similar manner to the main simulation, the mathematical models and the boundary conditions were implemented by *ANSYS* Fluent 14.0 following the same algorithm. The profiles for the flow variables: velocity, turbulent kinetic energy and dissipation rate of turbulent kinetic energy at the inflow boundary were coded by user-defined functions (*udf*) in the solver.

Results and Discussions

Results of the CFD Validation

The results of the validation of the *CFD* turbulence model are presented in Figs 8–10. Fig. 8 compares the simulation results of the mean stream wise wind velocity component at four locations on a vertical plane along the centreline of the building with the wind tunnel experimental data, while Fig. 9 compares the same velocity component at similar locations on a horizontal plane at y = 0.0125m (near the ground surface), for half domain. Fig. 10 shows the flow patterns around the building on the horizontal and vertical planes. While Fig. 10a depicts the ground-level vortex at the wind ward side of the building and the lee-eddy vertical recirculation behind the building, Fig. 10b shows the transverse ground-level double-eddy recirculation behind the building.

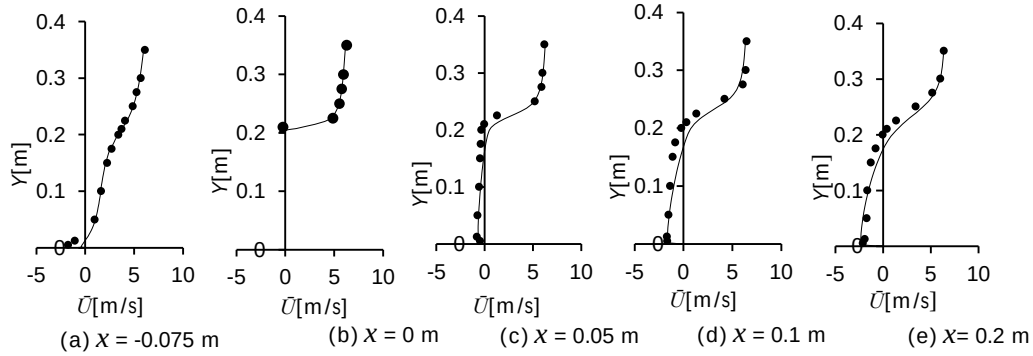

Fig. 8 Profiles of wind tunnel data (dotted points) and simulation results (solid lines) of mean streamwise wind velocity component,$\bar{U}$, on a vertical plane along building centreline

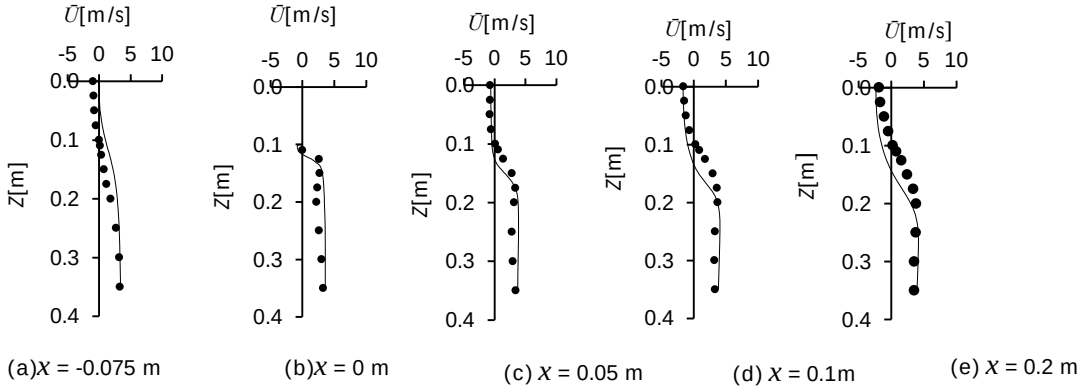

Fig. 9 Profiles of wind tunnel data (dotted points) and simulation results (solid lines) of mean streamwise wind velocity component, $\bar{U}$, on a horizontal plane at y = 0.0125m ($\frac{1}{16}h$)

It is observed from Fig. 8 that the simulation results for the mean streamwise wind velocity agree very well with the experimental data at the measuring points in front of and behind the building. The ground-level vortex at the wind ward side of the building and the lee-eddy vertical recirculations behind the building are also very well reproduced (Fig. 10a). However, it is noted from the figure that in the region

close to the building surface, the point of transition of the mean streamwise velocity from negative to positive values was calculated a little higher on the vertical axis. This may be due to the widely documented weakness of *RANS* models in slightly overestimation the size of the lee recirculation behind buildings, which causes the centre of the recirculation vortex to be shifted downwind and upwards.

From Fig. 9 it is shown that on the horizontal plane at y = 0.0125 m the model also satisfactorily reproduced the mean streamwise velocity. The transverse ground-level double-eddy recirculation behind the building is also very well represented (Fig. 10b). The same overestimation problem is also observed by the transition point of the calculated mean velocities being a little bit larger on the horizontal axis than the experimental data. The moderate deviation may also be due to the size of the recirculation eddy being larger than in the experiment, probably for the same reason mentioned before. It is observed, however, that in the far regions both on the vertical and horizontal planes, probably outside the recirculation zones, results are predicted more closely. It is believed therefore that the current *CFD* model has performed quite satisfactorily in predicting the flow field around the high-rise building model and as such is quite adequate for calculating the air ventilation performance of the two adjacent building configurations under investigation.

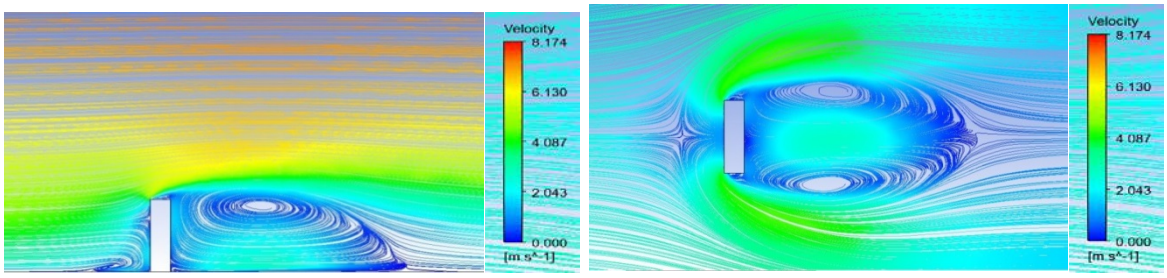

(a) (b)

Fig. 10 Recirculating eddies of the building model used for validation; (a) Recirculations on the vertical plane along the centreline of the building; (b) Transverse ground-level double-eddy recirculations behind the building. Direction of flow is from left to right.

It was also considered necessary to quantify the accuracy of the turbulence model and the numerical procedure adopted in studying the outdoor air ventilation around the adjacent buildings. Consequently, the experimental and calculated scalar wind velocities on the horizontal plane at y = 0.0125 m near the ground surface were compared quantitatively. Fig. 11 shows the graphical result of the comparison.

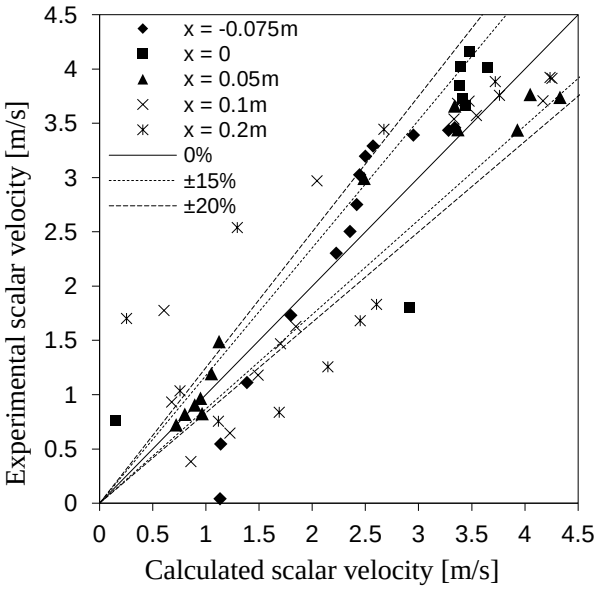

Fig. 11 Comparison of experimental scalar wind velocity data on a horizontal plane at y = 0.0125m with calculated results

From Fig. 11 it would be noted that majority of the results at the stronger wind regions (wind velocity > 2 - 2.5 m/s) outside the recirculation zones (From Figs 8 & 9, these generally corresponds to the region in the vertical direction defined by y > 0.2 m, and those regions in the transverse direction at z < –0.1 m and z > 0.1 m) predicted within 15% margin of error or 85% accuracy, while at the weak wind regions within the recirculation zones where the wind velocity is less than 2 m/s majority of the results are predicted to an accuracy of near 80%. The 15% error margin is normally considered highly accurate for the region where the wind speed is accelerated (Janssen *et al*., 2013).

The preceding analysis demonstrates that the current *CFDk–ε* turbulence model has performed quite well in predicting the flow field around the model of a single high-rise building. In engineering applications the 15% margin of error calculated for the scalar wind velocity relative to the experimental data is considered adequate (Cheung and Liu, 2011). The errors incurred by the calculations could be due to the assumption of isotropic turbulence stresses in the near-wall region made in the formulation of model. Errors might have also arisen as a result of the exact conditions of the measurement procedures which cannot be completely replicated by the *CFD* calculations. Some errors might have also been introduced due to interpolation inaccuracies for the flow and turbulence parameters at the inflow boundary. Some of these errors can be eliminated or reduced for better results by paying greater attention to how the simulation conditions are handled. Considering the overall performance, it was believed that the model is robust enough for predicting the air ventilation performance around the layout of two adjacent buildings.

Results of the Numerical Simulation

The results of the air ventilation characteristics of the various configurations of the layout of the two adjacent buildings are as presented in Figs. 12 and 13. Fig. 12 shows the variation of velocity ratio with the separation distance between the buildings, while Fig. 13 is the variation of dimensionless air exchange rate with the separation. The *HR* = 0 configuration indicated in the figures is for the reference case when there is no building adjacent to

the low-rise building at the downwind location.

From Fig. 12 it would be observed that velocity ratio generally increases with height ratio from *HR*=1.0 to *HR*=2.5. However, there is a sharp jump of *VR* from *HR*=1.5 to *HR*=2.0. It would also be observed that velocity ratio increases with separation distance up to a certain maximum for each height ratio before falling off to lower values with further increase in separating distance. This indicates that more air motion is induced at the pedestrian level as the height of the downwind building increases. This is in contrast to such building arrangement in which the upwind building has a greater height. In this step-up configuration, this may be due to the increased windward surface area of the downwind building channelling greater quantity of air down to the pedestrian level from the stagnation zone on the surface. For each of the height ratios, there is a separation distance at which the velocity ratio is highest. For *HR*=1.0 and *HR*=1.5 configurations, this maximum occurs at 18 m separation distance, while for *HR*=2.0 to *HR*=3.0 the maximum values occur at separation distance W_v=24 m. From the figure, it would also be seen that the maximum velocity ratio does not necessarily occur at *HR*=0; rather it occurs at *HR*>1.5 for each of the separation distances. This implies that air motion greater than obtainable for an isolated low-rise building could be induced when the low-rise building is adjacent to a downwind building with greater heights. This result is consistent with those reported in previous studies (Xie *et al*., 2005; Wang and Huang, 2006; Wang *et al*., 2006) even though the current research took into consideration the lateral flow phenomena such as street canyon axial advections and air exchanges across street openings associated with actual flows.

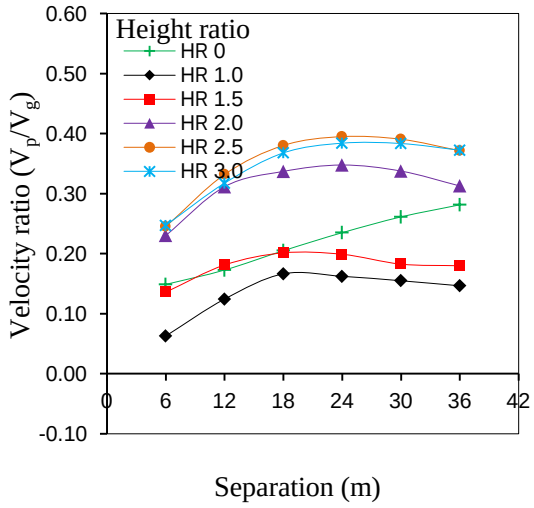

Fig. 12 Variation of velocity ratio with separation distance for different building height ratios

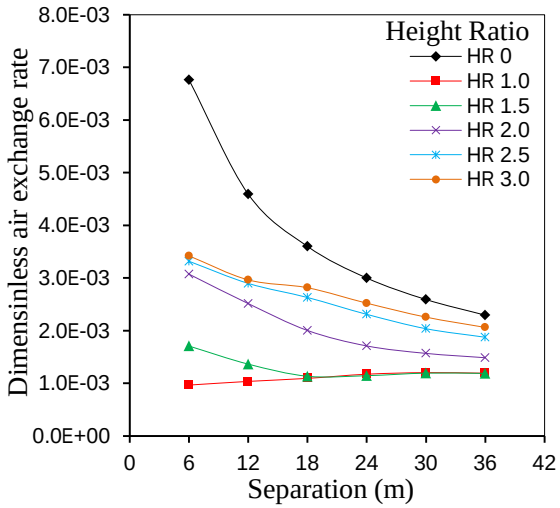

Fig. 13 Variation of dimensionless air exchange rate with separation distance for different building height ratios

Fig. 13 shows that the dimensionless air exchange rate generally increases with height ratio but decreases with separation distance except for *HR*=1.0 and *HR*=1.5 configurations. The first part of this result indicates that greater quantity of air from within the cavity between the buildings is exchanged with air from outside the cavity, which should result in better air quality. The result is consistent with that obtained for velocity ratio in Fig. 12. For *HR*=0 the exchange rate increases with separation distance, while for *HR*=1.5 it initially decreases with separation distance before

increasing mildly with the distance. From Fig. 13 it would be observed that the exchange rate for the reference case *HR*=0 is the greatest for each of the separation distances.

Based on the findings from the research, it is suggested that for the building layout and the configurations examined, at *HR*=1.0 a separation distance of 18 m could be adopted for air ventilation based on optimum air movement between the buildings at the pedestrian level. At *HR*=1.5 separation distances between 18 m and 24 could be used as the two distances offer the same ventilation performance. The choice can now be determined by other factors such as parking space and space for landscaping. However, between *HR*=1.0 and *HR*=1.5, W_v=18 m is to be maintained until very close to HR=1.5 when the choice between W_v=18 m and W_v=24 m can be made. At *HR*=2.0 a separation distance of 24 m is suggested, but can as well be 18 m or 30 m as these distances have very close ventilation performance to the maximum offered by the 24 m separation distance. Between *HR*=2.0 and the midway between *HR*=1.5 and *HR*=2.0, the separation distance can be 18 m or 24 m, but a separation distance of 30 m offers much lower ventilation performance. At *HR*=2.5 and between *HR*=2.0 and *HR*=2.5, a separation distance of 24 m is suggested though W_v=30 m may also be used for some other considerations. For the separation distances examined, between *HR* = 3.0 and the midway between *HR*=2.5 and *HR*=3.0, separation distances 24 m or 30 m may be used. It is be noted that where it was suggested that either of two separation distances may be used, it was implied that separation distances between the two choices are equally applicable.

Conclusion

The air ventilation characteristics of various step-up configurations of a layout of two adjacent buildings have been examined in this research work. Three-dimensional simulation of the flow by which effects of lateral turbulent flow features could be captured, and which utilize representative building geometry and actual wind data was conducted. The critical parameters studied are the separation distance between the buildings and buildings height ratio, and the air ventilation performance criteria adopted are wind velocity ratio and air exchange rate. It was shown that velocity ratio and dimensionless air exchange rate generally increase with height ratio. This indicates that more air motion is induced at the pedestrian level as the height of the downwind building increases, and greater quantity of air from within the cavity between the buildings is exchanged with air from outside the cavity, which could result in better air quality. For each of the height ratios, there is a separation distance at which the velocity ratio is highest. For *HR*=1.0 and *HR*=1.5, this maximum occurs at 18 m separation distance, while for *HR*=2.0 to *HR*=3.0 the maximum values occur at separation distance W_v=24 m. The results of the research demonstrate that an appropriate step-up configuration of two adjacent buildings can be used to enhance air motion at the pedestrian level of the buildings to enhance thermal comfort in a low-wind, hot and humid urban environment. The findings of the study further demonstrate the importance of giving consideration to relevant climatic elements in formulating guidelines for building layouts in an urban area. The findings can be of great benefits to urban planners and professionals in the building industry, particularly in urban environments similar to the one examined. The results may also find application in the area of heat transfer where the strategy may be applied to enhance the performance of a device like the extended surface employing annular fins by increasing the heights of successive fins serially in the downstream direction.

References

Ahmad, K.; Khare, M. and Chaudhry, K.K. (2005).Wind tunnel simulation studies on dispersion at urban street canyons and intersections—a review. *Journal of Wind Engineering and Industrial Aerodynamics*, Vol. 93, No. 9, 697-717.

Ansys, (2011). ANSYS Release 14.0. User's Guide. ANSYS Inc., Canonsburg.

ASHRAE, (1997). ASHRAE Handbook-Fundamentals, American Society of Heating and Air-Conditioning Engineers. Inc. Atlanta.

Ayo, S.A., Mohd-Ghazali, N. and Mansor, S. (2015). Outdoor ventilation performance of various configurations of a layout of two adjacent buildings under isothermal conditions. *Building Simulation*, Vol. 8, No. 1, 81-98.

Baik, J.-J. and Kim, J.-J. (1999). A numerical study of flow and pollutant dispersion characteristics in urban street canyons. *Journal of Applied Meteorology*, Vol. 38, No. 11, 1576-1589.

Blocken, B., Carmeliet, J. and Stathopoulos, T. (2007). CFD evaluation of wind speed conditions in passages between parallel buildings—effect of wall-function roughness modifications for the atmospheric boundary layer flow. *Journal of Wind Engineering and Industrial Aerodynamics*, Vol. 95, No. 9, 941-962.

Buccolieri, R., Sandberg, M., and Di Sabatino, S. (2010). City breathability and its link to pollutant concentration distribution within urban-like geometries .*Atmospheric Environment*, Vol. 44, No. 15, 1894-1903.

Chan, A.T., So, E.S.P. and Samad, S.C. (2001). Strategic guidelines for street canyon geometry to achieve sustainable street air quality. *Atmospheric Environment*, Vol. 35, No. 24, 4089-4098.

Cheung, J.O.P. and Liu, C. (2011). CFD simulations of natural ventilation behaviour in high-rise buildings in regular and staggered arrangements at various spacings. *Energy and Buildings*, Vol. 43, No. 5, 1149-1158.

Cook, N.J. (1990). The designer's guide to wind loading of building structures. Part 2, Static structures. 3rd Ed.

Fluent, Inc. (2005).Fluent 6.2 User's Guide. Fluent Inc., Lebanon, NH.

Franke, J. (2006). Recommendations of the COST action C14 on the use of CFD in predicting pedestrian wind environment. In: *The fourth international symposium on computational wind engineering*, Yokohama, Japan, 529-532.

Franke, J.; Hellsten, A.; Schlunzen, K.H. and Carissimo, B. (Eds.) (2008). Best practice guideline for the CFD simulation of flows in the urban environment. COST Action 732, quality assurance and improvement of microscale meteorological models, Brussels, COST office.

Franke, J.; Hirsch, C.; Jensen, A.G.; Krus, H.W.; Schatzmann, M.; Westbury, P.S.; Miles, S.D.; Wisse, J.A. and Wright, N.G. (2004). Recommendations on the use of CFD in wind engineering. In*: Proceedings of the International Conference on Urban Wind Engineering and Building Aerodynamics*, In*: van Beeck, J.P.A.J.(Ed.), COST Action C14, Impact of Wind and Storm on City Life Built Environment*, von Karman Institute, Saint-Genesius-Rode, Belgium. 5–7 May, 2004.

Hang, J., Li, Y. and Sandberg, M. (2011). Experimental and numerical sturdies of flow through and within high-rise building arrays and their link to ventilation strategy. *Journal of Wind Engineering and Industrial Aerodynamics*, Vol. 99, No. 10, 1036-1055.

Janssen, W.D.; Blocken, B. and van Hooff, T. (2013). Pedestrian wind comfort around buildings: Comparison of wind comfort criteria based on whole-flow field data for a complex case study. *Building and Environment*, Vol. 59, 547-562.

Leonard, B.P. (1979). A stable and accurate convective modelling procedure based on quadratic upstream interpolation. *Computer methods in applied mechanics and engineering*, Vol. 19, No. 1, 59-98.

Li, X.X.; Liu, C.-H.; Leung, D.Y.C. and Lam, K.M. (2006). Recent progress in CFD modelling of wind field and pollutant transport in street canyons. *Atmospheric Environment*, Vol. 40, No. 29, 5640-5658.

Liu, C.-H.; Barth, M.C. and Leung, D.Y. (2004). Large-eddy simulation of flow and pollutant transport in street canyons of different building-height-to-street-width ratios. *Journal of Applied Meteorology*, Vol. 43, No. 10, 1410-1424

Mills, G.; Cleugh, H.; Emmanuel, R.; Endlicher, W.; Erell, E.; McGranahan, G.; Ng, E., Nickson, A., Rosenthal, J. and Steemer, K. (2010). Climate information for improved planning and management of mega cities (needs perspective). *Procedia Environmental Sciences*, Vol. 1, 228-246.

Mochida, A.; Murakami, S. and Kato, S. (1994).The similarity requirements for wind tunnel model studies of gas diffusion. *Wind Eng. Japan*, Vol. 59, 23-28.

Ng, E.; Katzschner, L., Wang, U., Ren, C., and Chen, L. (2008).Working Paper No. 1A: draft urban climatic analysis map–urban climatic map and standards for wind environment–feasibility study. *Technical Report for Planning Department HKSAR*, Report No. WP1A, Planning Department of Hong Kong Government, Hong Kong.

Raupach, M.R.; Antonia, R.A. and Rajagopalan, S. (1991). Rough-wall turbulent boundary layers. *Applied Mechanics Reviews*, Vol. 44, No. 1, 1-25

Riain, C.M.N.; Fisher, B.; Martin, C.J. and Littler, J. (1998). Flow field and pollution dispersion in a central London street. *Environ. Monit.Assess*.,Vol. 52, 299–314.

Richards, P.J. andHoxey, R.P. (1993). Appropriate boundary conditions for computational wind engineering models using the k- ε turbulence model. *Journal of Wind Engineering and Industrial Aerodynamics*, Vol. 46, 145-153.

Santamouris, M.; Papanikolaou, N., Koronakis, I., Livada, I. and Asimakopoulos, D. (1999). Thermal and air flow characteristics in a deep pedestrian canyon under hot weather conditions. *Atmospheric Environment*, Vol. 33, No. 27, 4503-4521.

Tominaga, Y.; Mochida, A.; Shirasawa, T., Yoshie, R., Kataoka, H., Haromoto, K. and Nozu, T. (2004). Cross comparisons of CFD results of wind environment at pedestrian level around a high-rise building and within a building complex. *Journal of Asian Architecture and Building Engineering*, Vol. 3, No. 1, 63-70.

Tominaga, Y.; Mochida, A.; Yoshie, R.; Kataoka, H.; Nozu, T.; Yoshikawa, M. and Shirasawa, T. (2008). AIJ guidelines for practical applications of CFD to pedestrian wind environment around buildings. *Journal of Wind Engineering and Industrial Aerodynamics*, Vol. 96, 1749-1761.

Uehara, K.; Wakamatsu, S. and Ooka, R. (2003). Studies on critical Reynolds number indices for wind-tunnel experiments on flow within urban areas. *Boundary-Layer Meteorology*, Vol. 107, No. 2, 353-370.

Wang, J.-S. and Huang, Z. (2006). Numerical study on flow and dispersion in urban street canyons of asymmetrical configurations. *Journal of Hydrodynamics*, Ser. B, Vol. 18 No 3, Supplement), 146-150.

Wang, J.-S.; Zhao, B.-Q.; Ye, C., Yang, D.-Q.and Huang, Z. (2006). Optimizing layout of urban street canyon using numerical simulation coupling with mathematical optimization.*Journal of Hydrodynamics*. Ser. B, Vol. 18, No. 3, 345-351.

Wieringa, J. (1992). Updating the Davenport roughness classification. *Journal of Wind Engineering and Industrial Aerodynamics*, Vol. 41, No. 1, 357-368.

Xie, X.; Huang, Z. and Wang, J.-S. (2005). Impact of building configuration on air quality in street canyon. *Atmospheric Environment*, Vol. 39, No. 25, 4519-4530.

Xie, X.; Liu, C.-H.; Leung, D.Y.C. and Leung, M.K.H. (2006). Characteristics of air exchange in a street canyon with ground heating. *Atmospheric Environment*, Vol. 40, No. 33, 6396-6409.

Yim, S.H.L., Fung, J.C.H., Lau, A.K.H. and Kot, S.C. (2009).Air ventilation impacts of the “wall effect” resulting from the alignment of high-rise buildings. *Atmospheric Environment*, Vol. 43, No. 32, 4982-4994.

Yuan, C.; Ng, E. and Norford, L.K. (2014).Improving air quality in high-density cities by understanding the relationship between air pollutant dispersion and urban morphologies. *Building and Environment*, Vol. 71, 245-258.